

## Application of Ensemble Kalman Filter (EnKF) to Realistic Oil Sands Data

Yevgeniy V. Zagayevskiy and Clayton V. Deutsch

*This short note is devoted for application of data assimilation technique EnKF to realistic case study in order to constrain porosity and permeability distributions to hard well data and soft temperature measurements. The case study is carried out on adapted data from an Oil Sands Project in Northern Alberta (taken from public RMR reports). The results show improvement in estimation of geological properties of region around two well pairs, when any additional observation is integrated in the petroleum model, and can be extended to entire area of interest.*

### 1. Introduction

Proper quantification of geological properties of petroleum reservoir model leads to better management and improved oil recovery. Hard and/or soft data might be used in order to estimate distribution of porosity and permeability, key model parameters that dictate fluid flow in a reservoir. Inverse modeling technique for continuous data assimilation Ensemble Kalman Filter (EnKF) has been successfully applied number of times for characterization of a petroleum reservoir (Fahimuddin, 2010). Exhaustive temperature data from SAGD operated heavy oil fields in Northern Alberta may be coupled with EnKF to better understand geological architecture (Zagayevskiy and Deutsch, 2011). SAGD or assisted gravity drainage oil extraction method is based on injection of hot steam through upper horizontal well of a well pair and pumping heated oil from lower horizontal well. Once steam is injected in a reservoir, it starts occupying more and more space, what is called forming of a steam chamber, which grows upwards first and then sideways lowering viscosity of bitumen, which is in contact with hot agent, and forcing it to drain down due to gravity forces along steam chamber interface to production well (Butler, 1991). Since front of hot region is tightly related to steam (gas) saturation, change of temperature at specific location may be used to predict growth of steam chamber. Thus, temperature observations measured by thermal couples at surveillance wells may be used to describe geological properties of a reservoir.

Data are adapted here to examine influence of temperature assimilation through EnKF on estimation of porosity and permeability fields. It is relative new project, but with enough accumulated data. Benefit of use of additional soft data is presented by mean root squared error (MRSE) and mean of standard deviations of realization variations.

This short note is organized as follows. First a description of the project is presented. Geology and well layout are highlighted next to establish familiarity with the field. Then available temperature observations and porosity – permeability scatter plot are analyzed for creating basis of realistic case study. Estimates of porosity and permeability derived from using different data sets are compared and results are discussed.

### 2. Overview of Project

The case study is realistic, but synthetic because only publicly available information was considered. The case study is loosely organized after the Tucker reservoir is located in Northern Alberta, where Lloydminster is the closest large settlement (Figure 1). Lease area is presented on the same figure, which is not developed entirely, but only north-western part of it shown in red line. So far horizontal well pairs are drilled from three pads (A, B, and C) with varying number of wells: 8, 12, and 20 wells respectively (Figure 2). 350 MM bbl. of oil may be recovered from the field with daily production of 30,000 BOPD. Estimated ultimate recovery factor is about 55%. Oil is represented by bitumen with high viscosity and density of 9-10<sup>0</sup> API. For this reason 95% quality steam at 280 °C is injected into the reservoir in SAGD fashion. Production began in 2006 with three months of preheating procedure.

Reservoir is deposited in Clear Water formation, whose stratigraphy is shown in the Figure 3, approximately 500.0 m below the surface. It is argued that geology of the reservoir is formed by three stacked incised valleys created in deltaic environment and partially marine environment. Average thickness of net pay is 45.0 m. Average porosity and oil saturations are 0.31 and 0.56 respectively. Relationship between porosity and permeability is shown as scatter plot in the Figure 4. Cutoff value for permeability has been implemented at 10,000.0 mD. It is found that transform between these two variables is slightly different for different depositional environments, but generally in good correlation.

### 3. Data Analysis and Case Study Settings

Analysis of temperature data from observation wells shows change of temperature at only several wells, which are denoted by check mark (Figure 5). Region of working area around surveillance wells, at which observations show the change, is selected to use in modeling for characterization of porosity and permeability fields. Two well pairs of C pad with three observation wells are chosen for building a reservoir model, since change of temperature is the most at these wells, what is requirement of EnKF: increments of change of soft data values should be noticeable in time. Schematic of selected region is shown in the Figure 5, and change of observed temperature in time is shown in the Figure 6. It is clear that temperature changes only in surveillance wells #2 and #3, not in #1. Based on available information petroleum reservoir model is built, whose grid is presented in the Figure 7. Facies model built first consisting of permeable sand and impermeable shale, and the model is populated with porosity and permeability values describing both populations (sand and shale) with different parameters. Data of porosity, permeability and temperature after 540.0 days (18.0 months) of bitumen extraction are extracted at surveillance well locations. Histograms of base case and data may be found in the Figure 8 and Figure 9. Note that scatter plot of porosity and permeability should reproduce observed relationship between the same variables as shown in the Figure 4. Temperature observations are shown in the Figure 10. It is clear that even though they reproduce real spatial distribution of temperature, their values are smaller than actual ones.

### 4. Application of EnKF: Results

Theoretical background and implementation details on ENKF can be found in (Evensen, 2007; Zagayevskiy and Deutsch, 2011). Here five different case studies are worked out in order to investigate influence of incorporation of data type on estimation quality of porosity and permeability fields. Case studies are:

1. No data are used in estimation. Initial ensemble, which is generated based on the best knowledge of spatial continuity of porosity and permeability variables, represents the best estimate.
2. Porosity data from surveillance wells are integrated in the model.
3. Permeability data from same surveillance wells are assimilated in the model.
4. Porosity and permeability data are assimilated simultaneously.
5. Porosity, permeability and temperature data measured after 540.0 days production begins are used for estimation of porosity and permeability distributions.

The cases are compared through MRSE and  $\sigma$  values, whose expressions are shown below. Smaller values represent better quality of the model estimates. Comparison results are tabulated in the Table 1, which show that on average more assimilated data lead to better estimates. However, this is not always the case due to subjectivity of initial ensemble and representative level of available data. Graphically porosity best estimates are shown in the Figure 11.

$$RSE_{ireal} = \sqrt{\frac{\sum_{i=1}^{N_x} \sum_{j=1}^{N_y} \sum_{k=1}^{N_z} (z_{i,j,k}^{true} - z_{i,j,k,ireal}^{estimate})^2}{N_x \cdot N_y \cdot N_z}} \quad (1)$$

$$MRSE = \frac{\sum_{ireal=1}^{N_e} RSE_{ireal}}{N_e} \quad (2)$$

$$\sigma_{i,j,k} = \sqrt{\frac{\sum_{ireal=1}^{N_e} (z_{i,j,k,ireal}^{estimate} - \bar{z}_{i,j,k}^{estimate})^2}{N_e}} \quad (3)$$

$$\sigma = \sqrt{\frac{\sum_{i=1}^{N_x} \sum_{j=1}^{N_y} \sum_{k=1}^{N_z} \sigma_{i,j,k}^2}{N_x \cdot N_y \cdot N_z}} \tag{4}$$

where,  $z_{i,j,k}^{true}$  and  $z_{i,j,k}^{estimate}$  are the true and estimated values of a variable Z at location  $i, j, k$ ;  $\bar{z}_{i,j,k}^{estimate}$  is the average of estimates over realization at location  $i, j, k$ ;  $N_x, N_y$  and  $N_z$  are the number of blocks in X, Y, Z directions of a model.

**Table 1:** EnKF estimates quality with local update and shortcut. Number of realizations is 1000. Localization is applied for integration of temperature data.

Data Availability	Quality of Porosity Estimates		Quality of Permeability Estimates	
	MRSE	Std. Dev. $\sigma$	MRSE	Std. Dev. $\sigma$
No data	0.12083	0.10584	2417.2	1374.2
Porosity data	0.11895	0.10163	2399.5	1357.5
Permeability data	0.11938	0.10196	2366.9	1548.0
Porosity and permeability data	0.12118	0.09839	2373.7	1537.2
Porosity, permeability and temperature data	0.12097	0.09824	2372.2	1526.8

**5. Conclusion**

Influence of type and number of assimilated data on quality of estimates of porosity and permeability for realistic case study based on realistic data is presented in this short note. On average extra assimilated hard or soft data improve estimation results, but it is not always true, because of subjectivity of initial ensemble, comparison measures MRSE and  $\sigma$ , and representation level of available data. Further investigation of EnKF implementation details and more accurate study of properties of examined case study should be conducted in order to improve estimated distributions using given data at hand.

**References**

Butler, R., 1991, *Thermal Recovery of Oil and Bitumen*, Prentice Hall, Englewood Cliffs, New Jersey, 524 pp.  
 Deutsch, C.V. and Journel, A.G., 1998, *GSLIB: Geostatistical Software Library and User's Guide*, Oxford University Press, New York, 2nd Ed., 369 pp.  
 Evensen, G., 2007, *Data Assimilation: The Ensemble Kalman Filter*, Springer Verlag, Berlin, 305 pp.  
 Fahimuddin, A., 2010, 4D Seismic History Matching Using the Ensemble Kalman Filter (EnKF): Possibilities and Challenges, *PhD Thesis*, University of Bergen, Norway, 116 pp.  
 Husky Oil Operations Limited, 2010, *Annual Performance Presentation for Tucker Thermal Project (Commercial Scheme #9835)*, Energy Resources Conservation Board (ERCB), Calgary, 153 pp. Retrieved from [http://www.ercb.ca/portal/server.pt/gateway/PTARGS\\_0\\_0\\_321\\_0\\_0\\_43/http%3BercbContent/publishcontent/publish/ercb\\_home/industry\\_zone/industry\\_activity\\_and\\_data/in\\_situ\\_progress\\_reports/2010/](http://www.ercb.ca/portal/server.pt/gateway/PTARGS_0_0_321_0_0_43/http%3BercbContent/publishcontent/publish/ercb_home/industry_zone/industry_activity_and_data/in_situ_progress_reports/2010/)  
 Remy, N., Boucher, A. and Wu, J., 2009, *Applied Geostatistics with SGeMS: A User's Guide*, Cambridge University Press, New York, 264 pp.  
 Zagayevskiy and Deutsch, 2011, Temperature and Seismic Data Integration to a Petroleum Reservoir Model by Means of Ensemble Kalman Filter (EnKF), *Centre for Computational Geostatistics 13*, 209-1 – 209-24

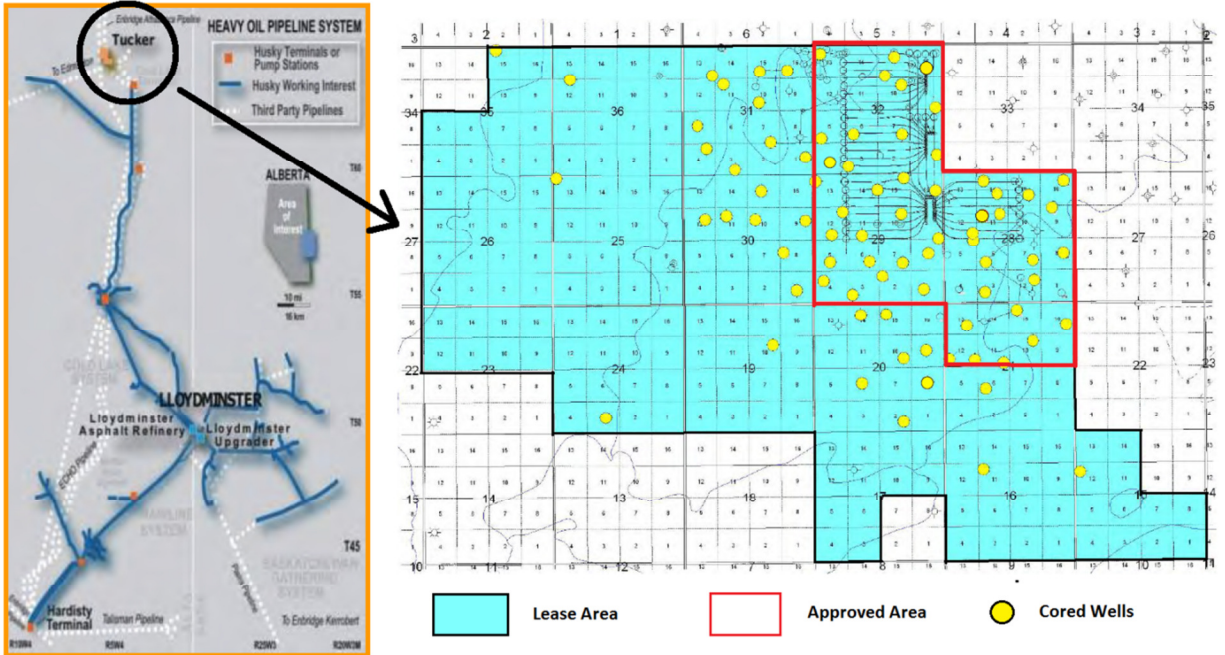


Figure 1: Location map and lease area of Tucker Project (Courtesy of Husky Energy)

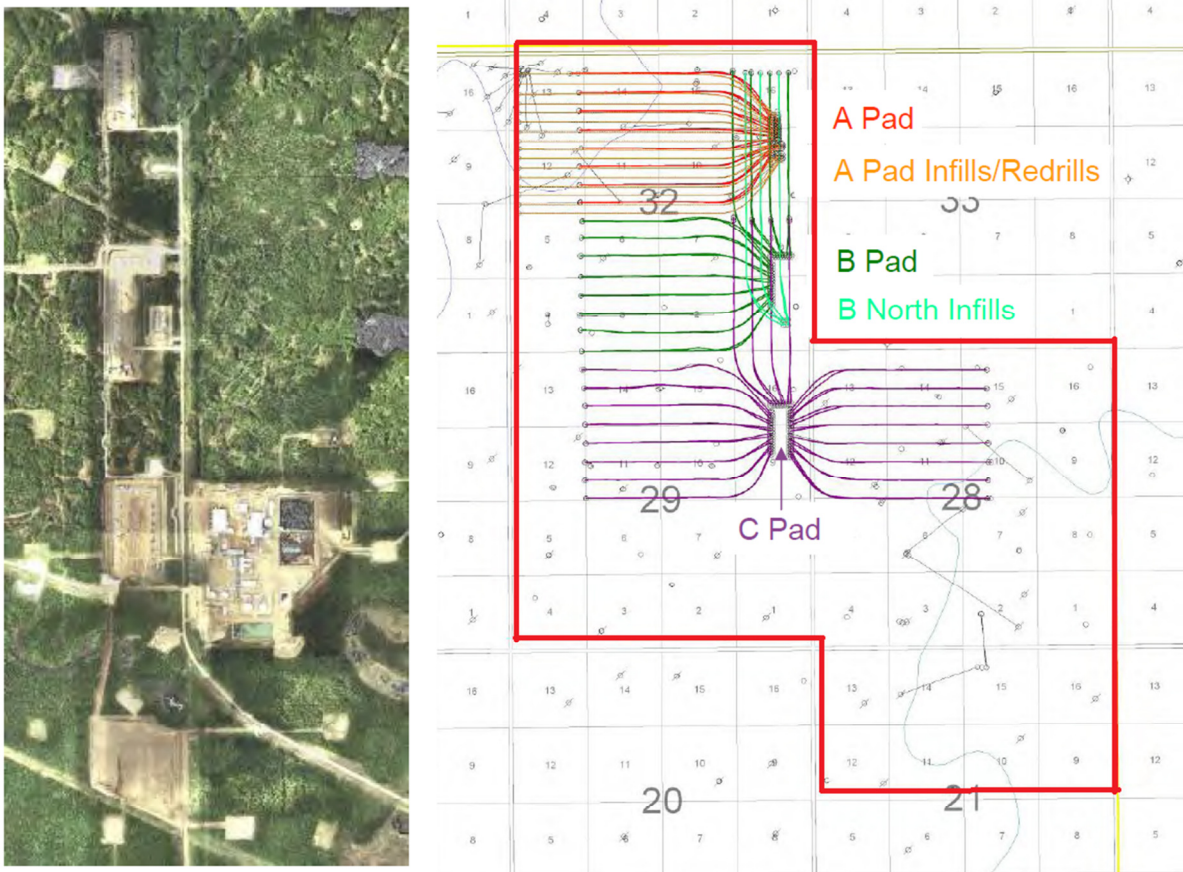


Figure 2: Aerial photo and approved area of Tucker Project with pads (Courtesy of Husky Energy)

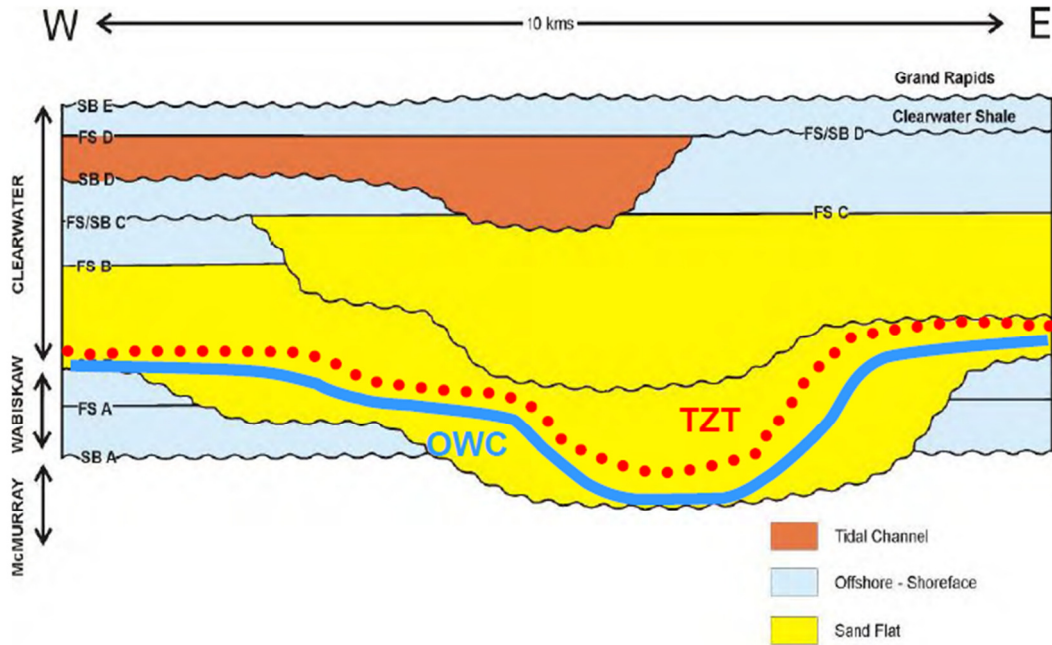


Figure 3: Stratigraphy of Tucker reservoir (Courtesy of Husky Energy)

Porosity-Permeability relationship for each valley over the project area based on the core data

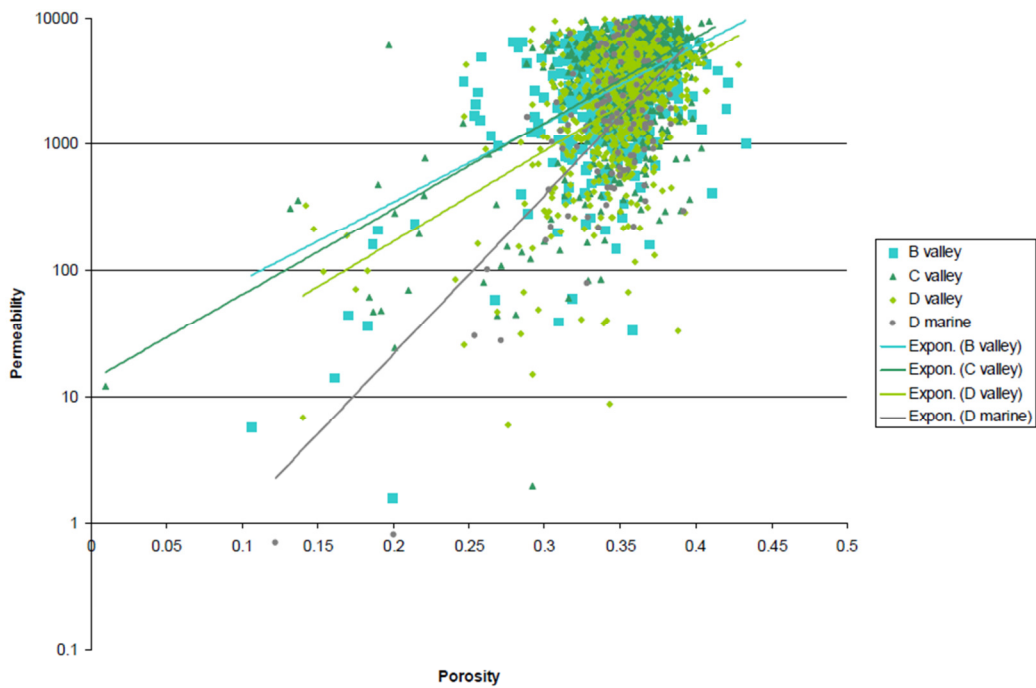


Figure 4: Porosity – permeability relationship from core analysis (Courtesy of Husky Energy)

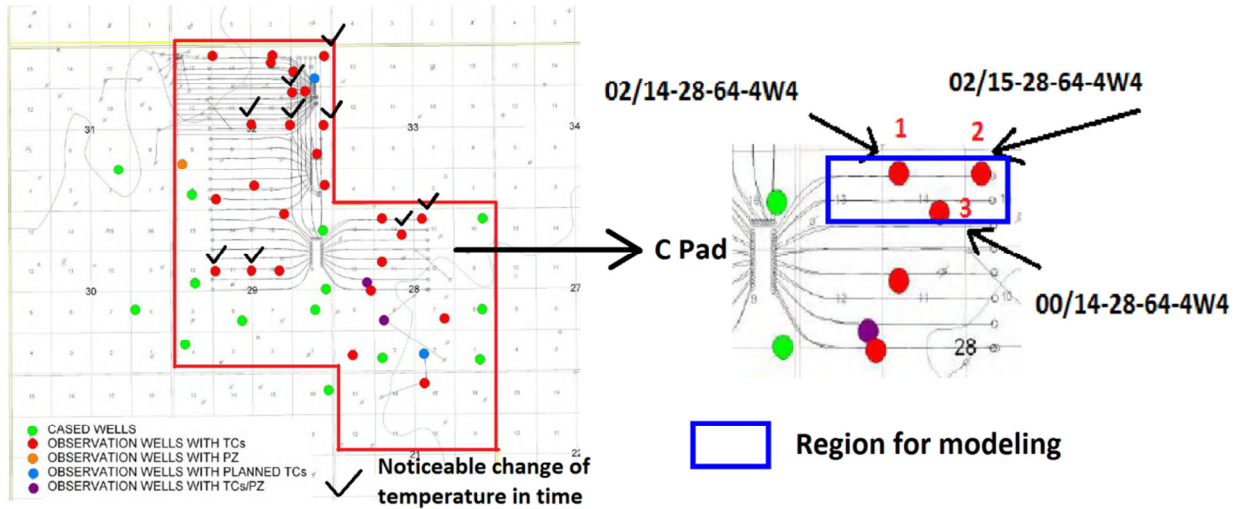


Figure 5: Location of observation wells and modeling region (Courtesy of Husky Energy)

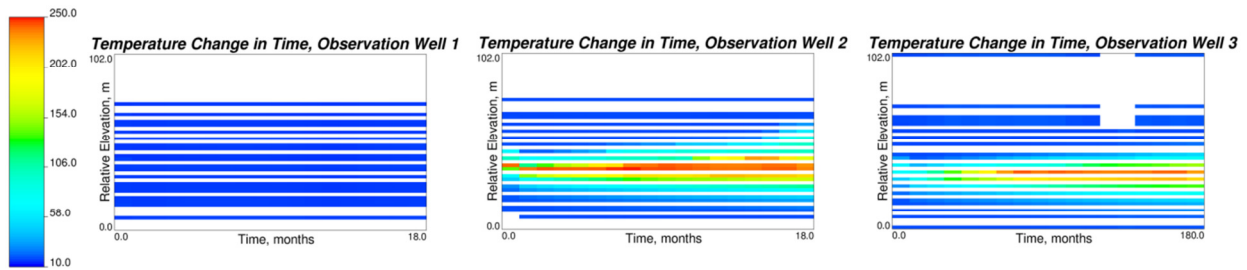


Figure 6: Observed change of temperature along observation wells 1, 2, and 3: 02/14-28-64-4W4, 02/15-28-64-4W4, and 00/14-28-64-4W4 (Courtesy of Husky Energy)

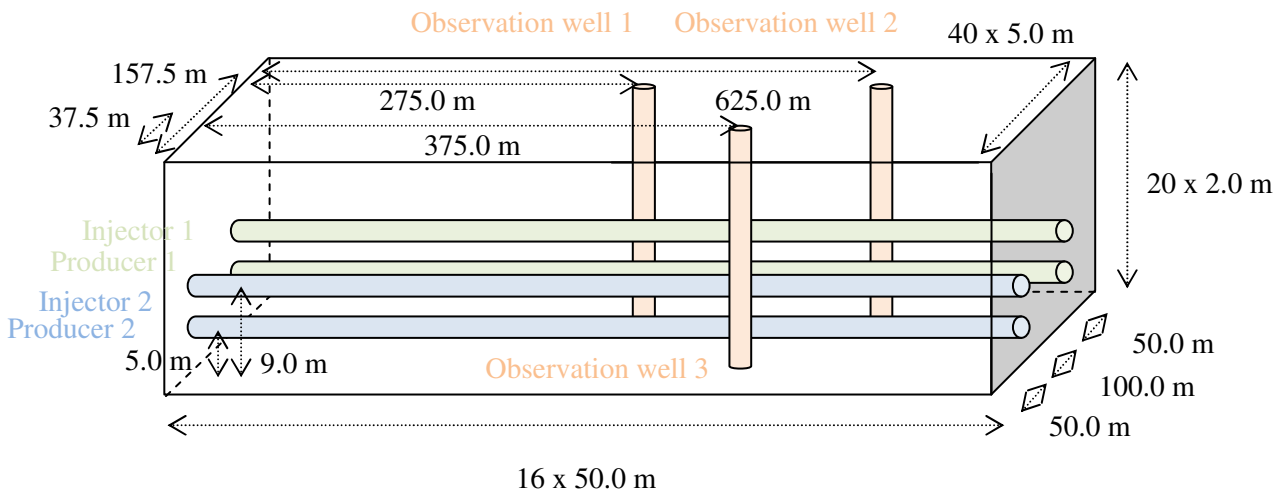
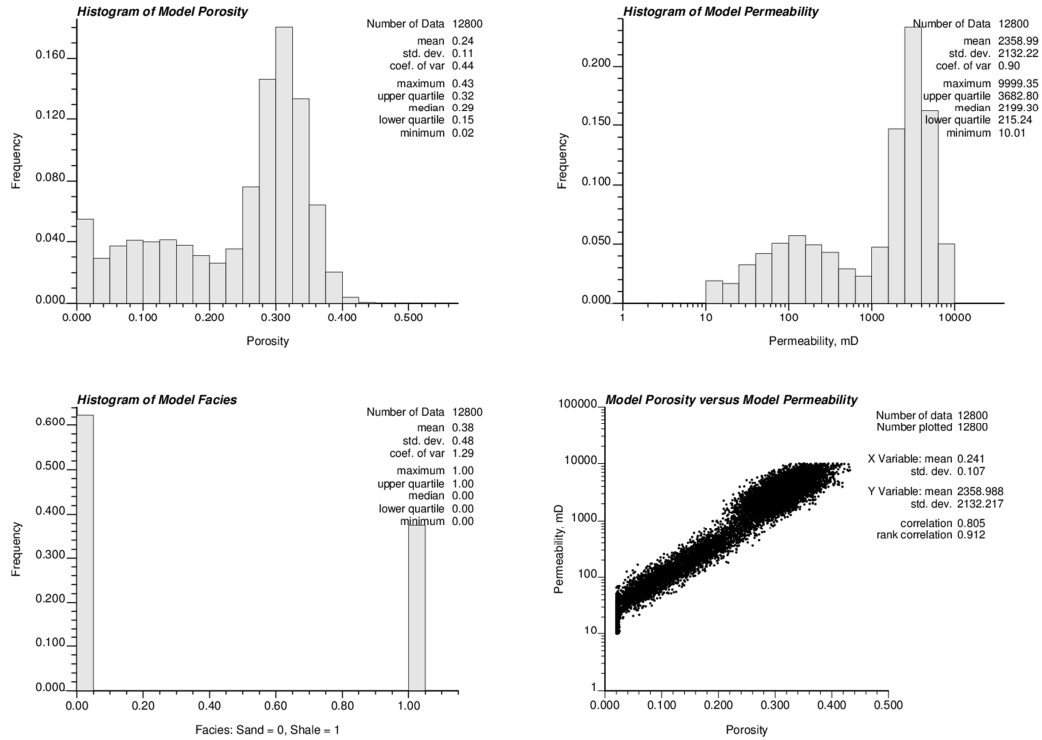
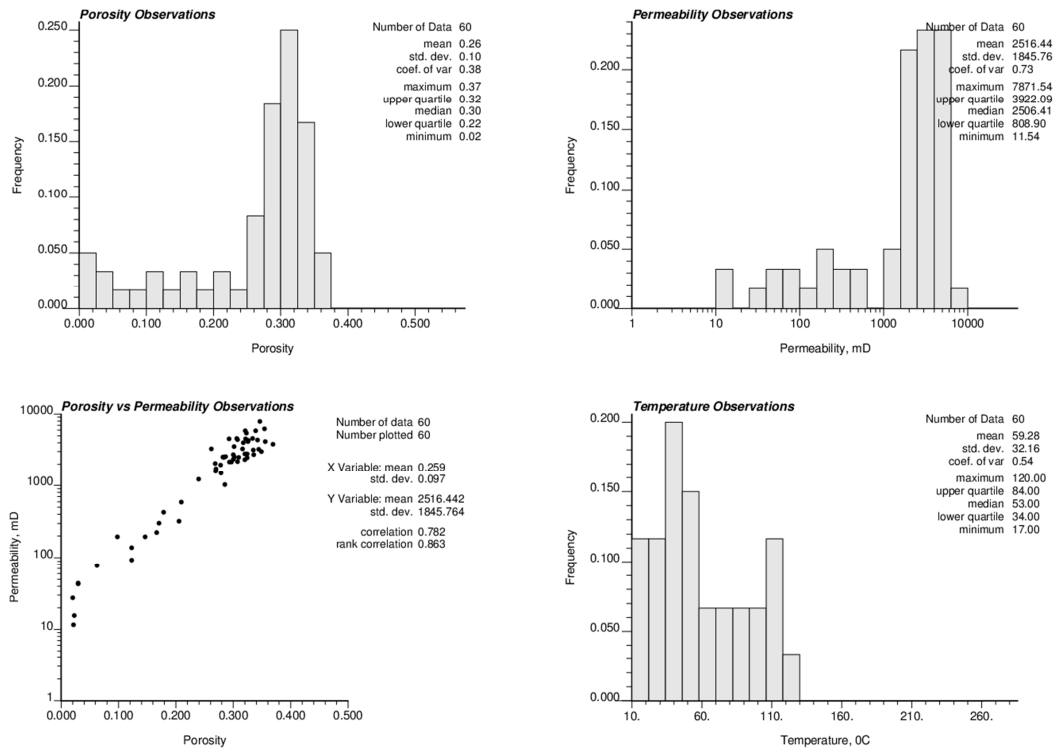


Figure 7: Schematic grid of the petroleum reservoir model and location of SAGD well pairs 1, 2 and observation wells 1, 2, and 3



**Figure 8:** Histograms of porosity, horizontal permeability and facies and scatter plot between porosity and permeability of realistically simulated base case of petroleum reservoir model



**Figure 9:** Histograms of observations of porosity, horizontal permeability and reservoir temperature and scatter plot between observations of porosity and permeability

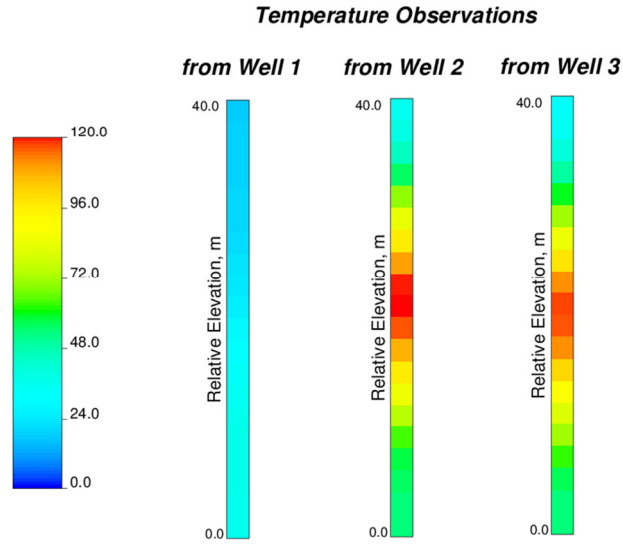


**Figure 10:** Temperature observations from surveillance wells used in modeling of porosity and permeability

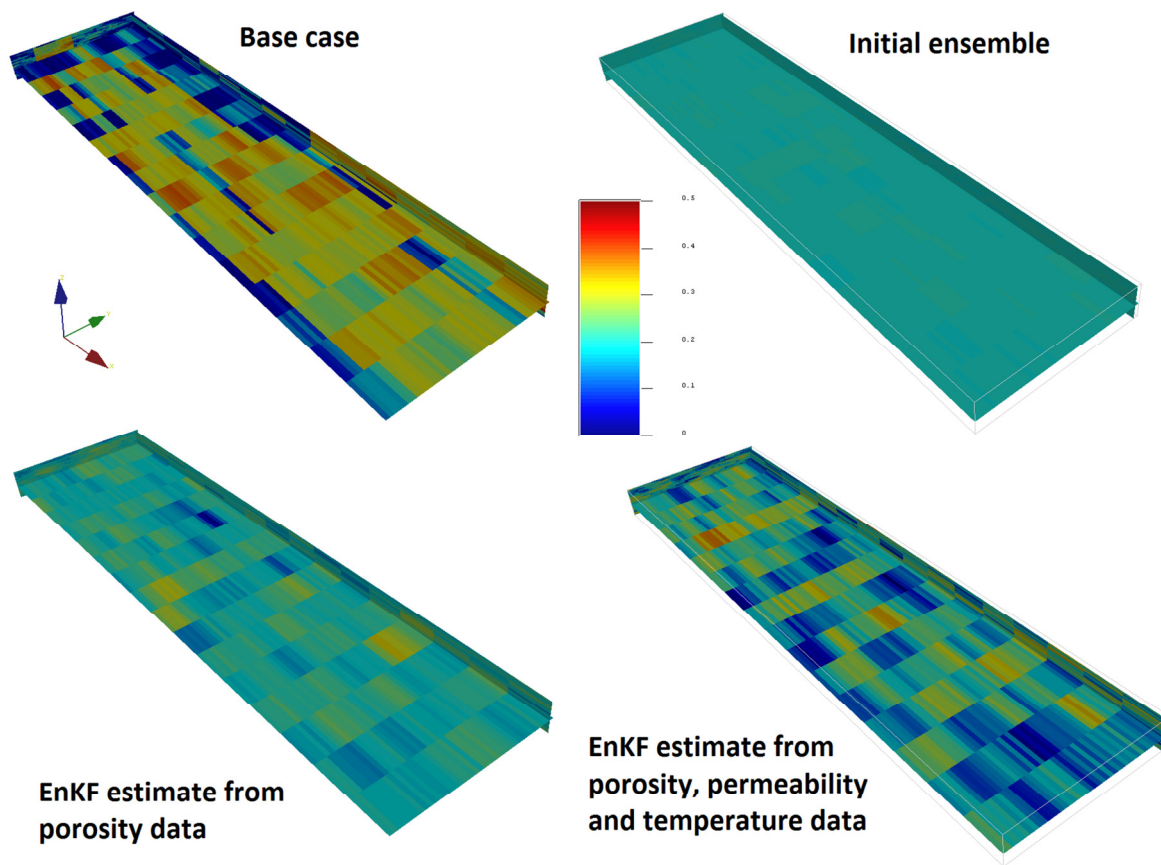


**Figure 11:** Porosity base case and mean of EnKF estimates derived using no data (initial ensemble), porosity data and porosity, permeability, and temperature data. Slice #8.